

MULTI-SPECTRAL TUNABLE EXCITATION FLUORESCENCE MICROSCOPY WITH A NANOIMPRINTED PDMS-ON-SILICON GRATING OPTICAL FILTER

N.-T. Huang, S. Truxal, Y.-C. Tung, and K. Kurabayashi
University of Michigan, Ann Arbor

ABSTRACT

We report a MEMS-based tunable grating optical filter device and its integration with a fluorescence microscope system. This integration allows for voltage-controlled wavelength tuning of excitation light from a multi-band source. We demonstrate the system's capability to selectively excite fluorescence protein molecules with different excitation/emission spectral characteristics using a chip of optical filter device arrays, each with a very small ($2\text{mm} \times 2\text{mm}$) footprint. The demonstrated technology has potential to enable massively-parallel multispectral fluorescence microscopy in biochip array settings.

INTRODUCTION

Multicolor fluorescence labeling is an important technique for biological applications, such as DNA sequencing [1], microarray screening [2] and multiplexed bead-based assay [3]. To achieve multispectral measurement, tuning the wavelength of excitation light is necessary. Conventional multispectral imaging systems normally use fluorescence light filtering devices, such as liquid crystal tunable filter (LCTF) and acousto-optical tunable filter (AOTF), for quick wavelength switching [4-6]. However, the switching speed of LCTFs is limited to the order of 20 Hz [7], which is not fast enough for optically tracking dynamic interactions of biomolecules. AOTFs can provide much faster speed ($\sim 100\text{kHz}$), but their large size and expensive cost limit their applications in lab-on-chip settings. To minimize the size and cost of wavelength tuning components, several microelectromechanical systems (MEMS)-based tunable gratings have been reported [8, 9]. However, these devices typically operate in the infrared band or have limited resolution in visible band, which make them inappropriate for use in tunable photoexcitation of fluorescently labeled probes. To address above problems, we have developed a polymer-on-silicon MEMS grating optical filter using polydimethylsiloxane (PDMS) as the grating material, which can achieve a larger wavelength tuning range compared to silicon-based equivalent devices. By integrating the PDMS grating device with a fluorescence microscope system, we demonstrate voltage-controlled wavelength tuning of a multi-band light source to excite cell-expressed multispectral fluorescence proteins

METHODOLOGY

The tunable optical filter developed here is a PDMS-on-silicon hybrid MEMS device constructed using the design concept and fabrication technique in our previous study [10, 11]. Figure 1(a) shows the optical image of a single grating device. The device consists of an optically transparent PDMS microbridge of $250\ \mu\text{m}$ in length and $150\ \mu\text{m}$ in width with a nanoimprinted grating

surface feature of $700\ \text{nm}$ in period. The detailed grating surface profile is shown in a SEM image (Figure 1(b)). The PDMS microbridge is bonded to a suspended silicon shuttle mass with a series of comb electrodes while its one end is fixed onto a substrate. To achieve wavelength tuning operation, the laser is aligned to pass through the grating bridge, as shown in Figure 1(c). The device is designed to yield a $\sim 45\ \mu\text{m}$ displacement to vary the diffraction angle of light at an optical wavelength bandwidth of $80\ \text{nm}$. Our previous work [10] shows the plasma-treated PDMS-silicon bonding is strong enough to sustain a 40% strain ratio and can operate over 100 million stretch cycles. The comb-drive is designed to have a tilted folded-beam silicon springs and a series of tapered arrangements of electrode finger. This design can minimize the nonlinear effects on the springs and electrostatic instability coming along with large comb-drive motions. Figure 1(d) shows a batch-fabricated array of 16 tunable grating optical filter devices on a $20\ \text{mm} \times 20\ \text{mm}$ chip. The whole device is mounted on a carrier board by wire bonding, which would enable massively-parallel voltage-controlled wavelength tuning.

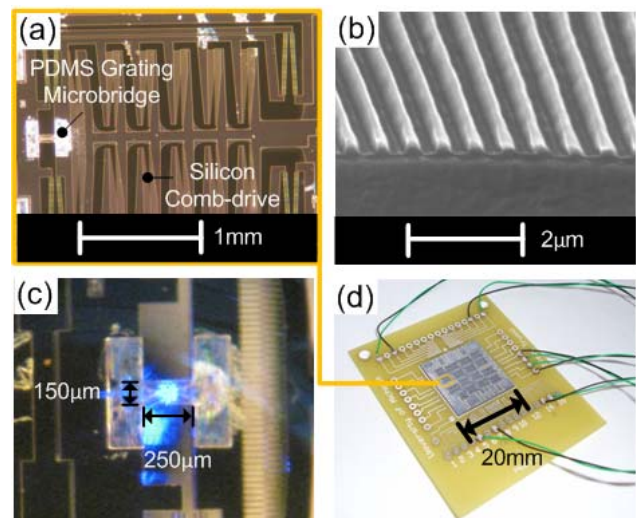


Figure 1: Images of nanoimprinted grating optical tunable filter. (a) Optical image of single grating unit. (b) SEM image of $15\ \mu\text{m}$ -thick PDMS microbridge with $700\ \text{nm}$ nominal pitch. (c) Blue laser ($\lambda = 473\ \text{nm}$) passing through $250\ \mu\text{m} \times 150\ \mu\text{m}$ grating bridge. (d) Whole 16 device array chip ($20\ \text{mm} \times 20\ \text{mm}$) mounted to carrier board with wires.

Figure 2(a) shows the working principle of the grating device. The wavelength tuning is performed by varying the PDMS grating pitch a with the silicon comb-drive actuated by a voltage signal. The incident light along with the z-direction is passing through the optical transparent grating in the x-y plane. The grating equation can be written as:

$$\lambda = a (\sin\theta_1) \quad (1)$$

where λ is one incident light wavelength, a is the initial grating period and θ_1 is the first order diffraction angle of λ . When introducing a mechanical strain to elongate the spatial period of the grating to a' , the wavelength of the first order diffraction at the same angle θ_1 will shift from λ to λ' . The corresponding mechanical strain ε can be defined as:

$$\varepsilon = \frac{a' - a}{a} = \frac{\lambda' - \lambda}{\lambda} \quad (2)$$

The relation between the wavelength shift $\lambda' - \lambda$ and the mechanical strain can be given by $\lambda' - \lambda = a\varepsilon \sin \theta_1 = \lambda\varepsilon$. From this relation, the wavelength shift of the first order diffraction at the angle θ_1 is linearly proportional to the mechanical strain introduced to the grating structure. At an actuation voltage of 180V, the grating strain level can increase up to 18%, which corresponds to a wavelength tuning range of 80nm in the visible wavelength band (Figure 2(b)). Due to a stress-softening phenomenon in the elastic material, the grating strain increases rapidly in higher actuation voltage.

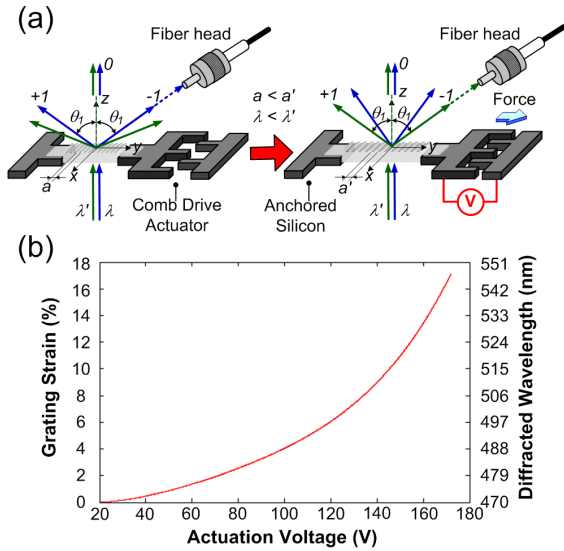


Figure 2: Working principle of the grating device. (a) Device operation principle. The actuator is stretched by an actuation voltage. (b) Relationship between the comb-drive actuation voltage and the grating strain/diffracted wavelength.

To study the wavelength tuning capability and spectral resolution of the grating device, it is integrated into a fluorescent microscope setting (Nikon Eclipse TS100, Nikon Inc.) with blue ($\lambda=473\text{nm}$), green ($\lambda=532\text{nm}$) and yellow ($\lambda=594\text{nm}$) laser (BWB-475-4E, BWB-532-10E, B&W TEK and Rigel Series Yellow, Laserglow) as incident lights passing through its PDMS bridge. The setup is illustrated in Figure 3. A 0-180V actuation voltage applied to the grating device is generated from a function generator and a voltage amplifier. A fiber probe with a $1000\mu\text{m}$ diameter core (A57-746, Edmund Optics Inc.) is used to capture the diffraction light. A three-color wavelength tuning spectrum is measured by an optical spectrometer (USB4000, Ocean Optics Inc.). The dual-color fluorescent image of a mixture of fluorescence protein-expressing prostate cancer cells is monitored by a

CCD camera, which is coupled with a 10x objective. A 500 nm long pass filter (S-003767, Chroma) and 532 nm notch filter (NF01-532U-25, Semrock) are used to eliminate the excitation laser light.

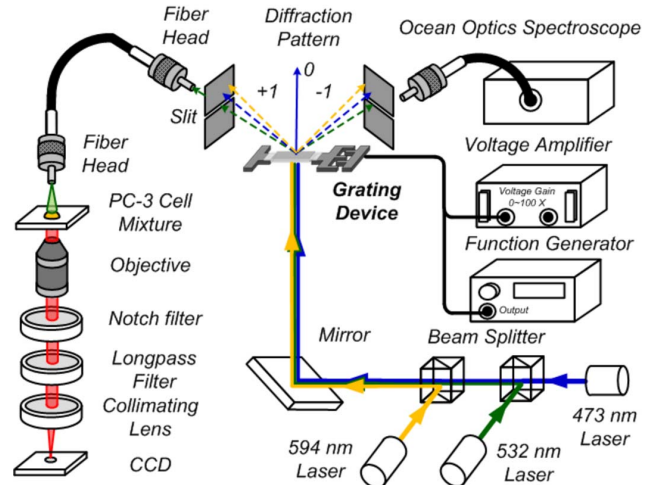


Figure 3: Schematic of optical setup for tuning three-color excitation laser and for imaging green/red fluorescence protein (GFP/RFP)-expressing PC-3 prostate cancer cells.

RESULTS AND DISCUSSIONS

Figure 4(a) and 4(b) show spectra of dual-color laser excitation controlled by our voltage-controlled MEMS tunable grating optical filter device. These excitation spectra were measured using the optical spectrometer. By varying the actuation voltage from 0-180V, the diffraction light wavelength channeled at a fixed angle changed from a

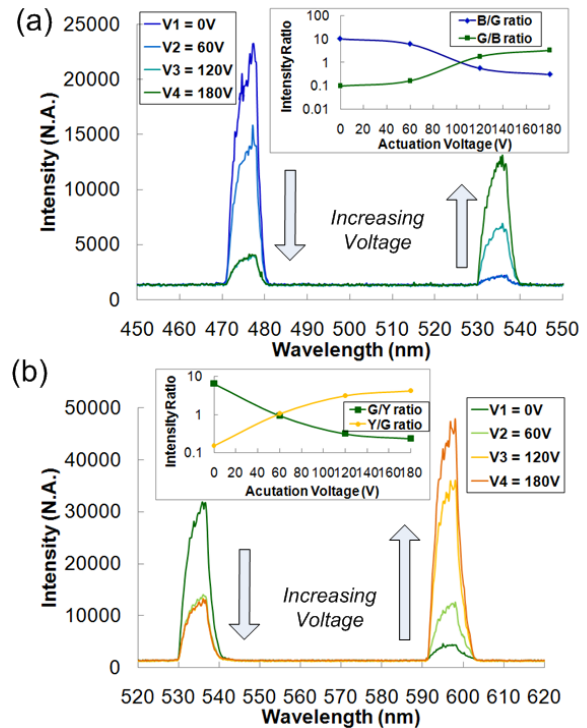


Figure 4: MEMS grating optical filter-controlled dual-color laser excitation spectra measured by optical spectrometer. The (a) blue ($\lambda = 473\text{nm}$) and green ($\lambda = 532\text{nm}$) and (b) green ($\lambda = 532\text{nm}$) and yellow ($\lambda = 594\text{nm}$) laser intensity combinations are varied by the actuation voltage. The inset figure shows the intensity ratio. The spectral resolution estimated from the FWHM of the spectral peaks is $<10\text{ nm}$.

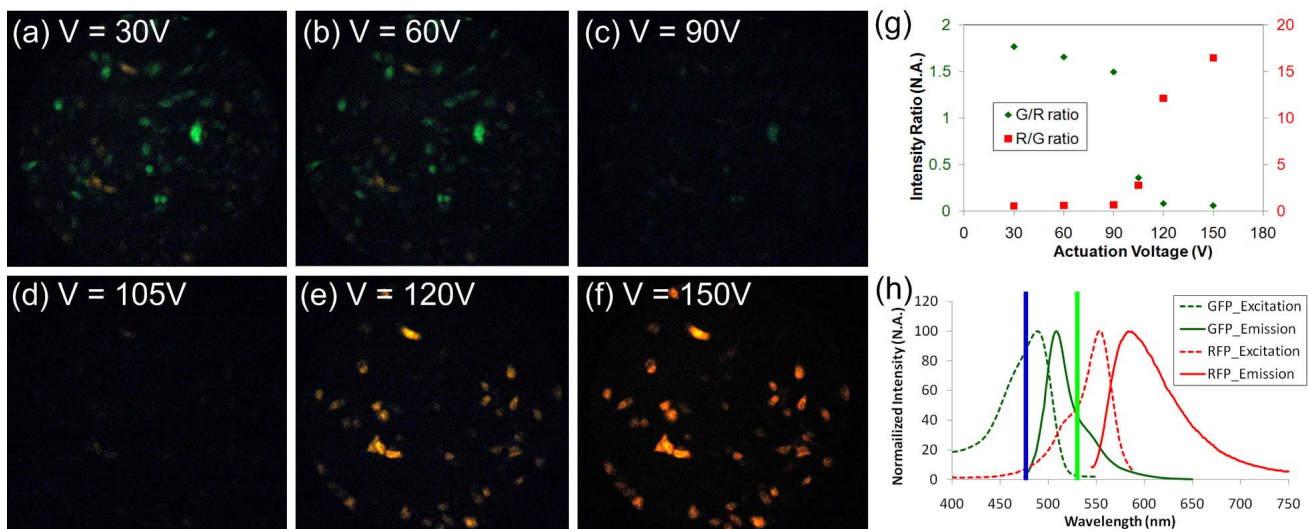


Figure 5: Tunable photoexcitation of mixed population of GFP/RFP-expressing PC-3 prostate cancer cells our MEMS grating optical filter device. (a)-(f) Sequential images of two-color emissions at increasing voltage (g) Fluorescent intensity ratio as a function of the actuation voltage applied to the grating device. (h) Excitation and emission spectra of GFP and RFP. The blue (green) line represents the 473nm (532nm) laser spectral peak.

lower to higher value. The insets of Figure 4(a) and 4(b) show that the corresponding dual-color laser intensity ratio varies from 10 to 0.1. With the diffraction angle adjusted by changing the positions of the slit and fiber probe, the wavelength band was tuned from 465-545nm to 525-610nm. If three or more color laser excitation tuning is required, we can double the wavelength range up to 200nm by adding another set of slit and fiber probe on the opposite side with respect to the z-axis.

To demonstrate the excitation light modulation by the grating device for cell imaging, we selected a mixed population of green and red fluorescent protein (GFP/RFP)-expressing PC-3 prostate cancer cells. Here, PC-3 cells maintained in complete media consisting of RPMI-1640 (61870, Gibco) supplemented with 10% (v/v) fetal bovine serum (FBS, 10082, Gibco), and 1% (v/v) antibiotic-antimycotic (15240, Invitrogen).

Figure 5(a)-(f) constitute an image sequence of cell mixture excited at different intensity ratios of two laser wavelengths (473nm and 532nm) controlled by the actuation voltage. Using ImageJ software, the GFP/RFP emission intensity ratio was obtained for a single cell, as shown in Figure 5(g). At the actuation voltage $V=30V$, the green/red ratio is 1.77. As the actuation voltage increases from 60 to 120V, the green/red ratio drops (alternatively, a red/green ratio increases). It represents the device's ability to continuously tune the excitation light color ratio. At $V=150V$, the red/green ratio is 16.45, which shows that most of the RFP-expressing cells are excited by green laser. The lower green/red intensity ratio at $V=30V$ is attributed to the broader excitation band of RFP at the shorter wavelength region. The 473nm laser still partially excites the RFP-expressing cells. Figure 5(h) shows the excitation and emission spectra of GFP and RFP. Our imaging system is limited by the CCD camera's speed of 30Hz. Therefore, although the device can be actuated at $>1kHz$, it was operated at a low actuation frequency ($\sim 1Hz$) during the imaging of the fluorescently labeled cells in this study. For fast multispectral cell image capture, we can replace current camera to a high-speed CCD camera or a

multiple-anode photomultiplier tube (PMT).

Like other tunable optical filter techniques, the MEMS-based grating optical filter device could be used in alternating laser excitation (ALEX). ALEX is a fast dual excitation wavelength tuning method that can be used to advance single-molecule fluorescence resonance energy transfer (FRET) measurements. In current FRET measurement, it is difficult to differentiate low FRET samples consisting of a donor(B)-acceptor(G) pair with an inter-distance longer than 8nm from those of only a donor(B), like case 2 and case 4 in Figure 6(a) (both have low FRET efficiency). Because ALEX allows dual donor and acceptor excitation, it can provide complete information on the presence and state of both donor and acceptor fluorophores [12]. Another application of ALEX is resolving conformational changes and intermolecular interactions of multiple biological molecules. It usually cannot be resolved by one donor-one acceptor fluorophore FRET [13]. As shown in Figure 6 (b), by quasi-simultaneously exciting two FRET combinations (B-Donor/G,R-Acceptor, and G-Donor/R-Acceptor) with a fast excitation tuning speed, the real-time FRET efficiency (E_{BG} , E_{BR} and E_{GR}) can be obtained to resolve time-dependent distance of three molecules (e.g. localizing RNA polymerase on DNA) [14].

Although ALEX adds important capabilities to the single-molecule FRET, its inherently complicate and time-consuming measurement process limits its throughput. Therefore, we propose to build up an optical system with MEMS-based grating optical filter array for massively-parallel alternating laser excitation (MP-ALEX). As illustrated in Figure 6(c), dual-color laser light from an excitation source coupled with a fiber bundle and a pinhole array passes through a grating array. The miniature size ($\sim 4mm^2$) of the individual device can diffract the light and excites each site of the sample array on the substrate. The grating device allows for high-speed spectral tuning within 0.5ms [15], which is fast enough to simultaneously monitor real-time conformational changes of biological molecules and intermolecular interactions at different sample sites.

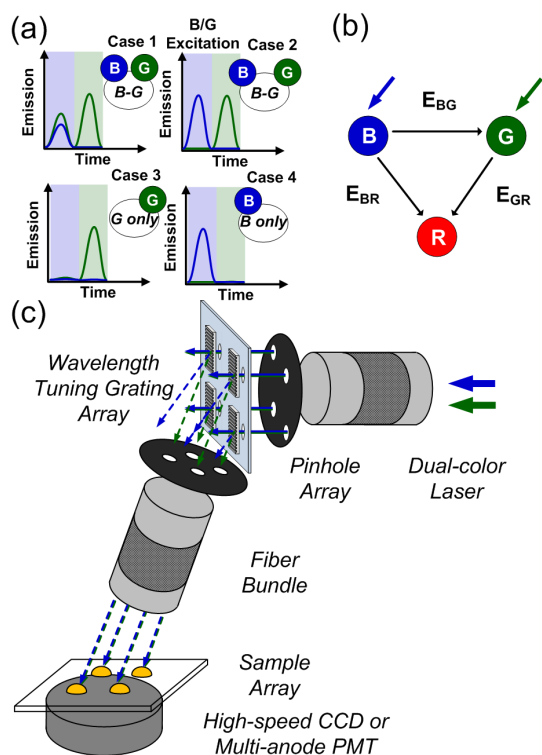


Figure 6: High-speed dual-color ALEX for detecting (a) 4 different molecular binding states and (b) a time-dependent distance of 3 molecular probes. (c) Concept of massively-parallel alternating laser excitation (MP-ALEX) enabled by the MEMS tunable grating optical filter array for high-throughput multi-probe FRET.

CONCLUSIONS

In summary, we have developed a visible wavelength tuning technique by a MEMS-based grating optical filter device. The device consists of a nanoimprinted elastic PDMS grating structure and silicon comb-drive with tapered electrode fingers allowing for large displacement and high-speed actuation. By integrating the device with a fluorescence microscope, we have demonstrated voltage-controlled excitation wavelength tuning from a multi-band light source. The system can selectively excite cell populations expressing fluorescence proteins with different excitation/emission spectral characteristics. Because of the miniature size of each grating device, we could build the optical grating filter array with a small foot print, which would enable massively-parallel multispectral fluorescence microscopy in lab-on-chip settings.

ACKNOWLEDGEMENTS

The authors thank Prof. Shuichi Takayama and Dr. Amy H. Hsiao at the University of Michigan Biomedical Engineering Department for their advice on cell preparation and experiment design. This work was supported by NSF under the grant No. ECCS-0601237.

REFERENCES

[1] K. M. O'Brien, J. Wren, V. K. Davé, D. Bai, R. D. Anderson, S. Rayner, G. A. Evans, A. E. Dabiri, H. R. Garne, "A hyperspectral imaging DNA sequencer", *Rev. Sci. Instrum.*, vol. 69, pp. 2141-2146, 1998.

[2] J. A. Timlin, "Scanning microarrays: current methods and future directions" *Methods Enzymol.*, vol. 411, pp.

79-98, 2006.

[3] J. P. Nolan, L. A. Sklar, "Suspension array technology: evolution of the flat-array paradigm", *Trends Biotechnol.*, vol. 20, pp. 9-12, 2002.

[4] H. R. Morris, C. C. Hoyt, P. J. Treado, "Image Spectrometers for fluorescence and raman microscopy- acousto-optic and liquid crystal tunable filters", *Applied Spectroscopy*, vol. 48, pp. 857-866, 1994.

[5] L. Bei, G. I. Dennis, H. M. Miller, T. W. Spaine, J. W. Carnahan, "Acousto-optic tunable filters: fundamentals and applications as applied to chemical analysis techniques," *Progress in Quantum Electronics*, vol. 28, pp. 67-87, 2004.

[6] J. Vila-Frances, J. Calpe-Maravilla, J. Munoz-Mari, L. Gomez-Chova, J. Amoros-Lopez, E. Ribes-Gomez, V. Duran-Bosch, "Configurable-bandwidth imaging spectrometer based on an acousto-optic tunable filter," *Review of Scientific Instruments*, vol. 77, 2006.

[7] N. Gat, "Imaging spectroscopy using tunable filters: A review," in *Proc. SPIE – Wavelet Applications VII.*, vol. 4056, pp. 50-64, 2000.

[8] H. Sagberg, M. Lacolle, I. Johansen, O. Lvhaugen, R. Belikov, O. Solgaard, A. S. Sudb, "Micromechanical Gratings for Visible and Near-Infrared Spectroscopy", *IEEE J. Sel. Top. Quantum Electron.*, vol. 10, pp. 604, 2004.

[9] Y. Wang, Y. Kanamori, T. Sasaki, K. Hane, "Design and fabrication of freestanding pitch-variable blazed gratings on a silicon-on-insulator wafer", *J. Micromech. Microeng.*, vol. 19, pp. 025019, 2009.

[10] S. C. Truxal, Y. -C. Tung, K. Kurabayashi, "A Flexible Nanograting Integrated Onto Silicon Micromachines by Soft Lithographic Replica Molding and Assembly," *J. Microelectromechanical Systems.*, vol. 17, pp. 393-401, 2008.

[11] S. C. Truxal, Y. -C. Tung, K. Kurabayashi, "High-Speed Deformation Soft Lithographic Nano Grating Patterns for Ultrasensitive Optical Spectroscopy", *Appl. Phys. Lett.*, vol. 92, pp. 05116, 2008.

[12] Y. Santoso, L.C. Hwang, L. L. Reste, A. N. Kapanidis "Red light, green light: probing single molecules using alternating-laser excitation", *Biochem. Soc. Trans.*, vol., 36, pp. 738-744, 2008.

[13] S. Hohng, C. Joo, T. Ha, "Single-molecule Three-color FRET", *Biophys. J.*, vol. 87, pp. 1328-1337, 2004.

[14] N. K. Lee, A. N. Kapanidis, H. R. Koh, Y. Korlann, S. O. Ho, Y. Kim, N. Gassman, S. K. Kim, S. Weiss, "Three-Color Alternating-Laser Excitation of Single Molecules: Monitoring Multiple Interactions and Distances", *Biophys. J.*, vol. 92, pp. 303 - 312, 2007.

[15] N. -T. Huang, S. C. Truxal, Y. -C. Tung, A. Y. Hsiao, G. D. Luker, S. Takayama, K. Kurabayashi, "Multiplexed Spectral Signature Detection for Microfluidic Color-Coded Bioparticle Flow", *Anal. Chem.*, vol. 82, pp. 9506-9512, 2010.

CONTACT

*N.-T. Huang, tel: +1-734-7630958; nthuang@umich.edu